A New Determination of the Shear Modulus of the Human Erythrocyte Membrane Using Optical Tweezers

Sylvie Hénon, Guillaume Lenormand, Alain Richert, and François Gallet
Laboratoire de Biorhéologie et d'Hydrodynamique Physico-Chimique, ESA 7057 associée au CNRS et aux Universités Paris 6 et Paris 7, 75251 Paris cedex 05, France

ABSTRACT Optical tweezers are used to apply calibrated forces to human erythrocytes, via small silica beads bound to their membrane. The shear modulus μ of the membrane is inferred from measurements of the cell deformation in the small strain linear regime. We find the same result $\mu = 2.5 \pm 0.4$ μN/m for both discotic and nearly spherical swollen cells. This value is smaller than the one deduced from micropipettes experiments. However the two methods do not operate in the same deformation regime and are not expected to lead to the same result.

INTRODUCTION

In this work, optical tweezers are used for the first time to measure the elastic coefficients of the red blood cell membrane. The recent development of this technique has opened new possibilities for convenient manipulation of biological objects (Svoboda and Block, 1994). Optical tweezers make it possible to trap, manipulate, and displace a living cell or a part of it without damage, either directly or using specific handles (Ashkin et al., 1987; Block et al., 1989; Visscher et al., 1993; Vorobjev et al., 1993; Dai and Sheetz, 1995). Moreover, this tool can be made quantitative after a careful calibration (Simmons et al., 1996; Svoboda and Block, 1994); the restoring force in the trap depends on the size, the shape, and the optical index of the trapped object and is proportional to the incident light power. Typical values of escape forces lie between 1 and 50 pN, which is in the range necessary to locally distort a cell.

Direct red blood cell trapping has been reported in the literature (Ashkin et al., 1987; Svoboda et al., 1992; Bronkhorst et al., 1995; Mammen et al., 1996). In an experiment using multiple trapping, the cell was seized by three points and deformed into a parachute shape (Bronkhorst et al., 1995). Then the relaxation time to equilibrium was measured, which is a combination of the membrane elastic moduli and viscosities. However, this configuration did not allow the authors to measure the membrane elastic coefficients, because the trapped volume and thus the exerted force were not well defined.

In this work we report simultaneous measurements of forces and deformations exerted on a red blood cell, from which we infer the elastic shear modulus of the membrane. The cell is seized and deformed by means of two small silica beads bound to the membrane. The beads are trapped in split optical tweezers and used like handles to pull on the membrane with two opposite forces, which are determined by a preliminary calibration.

We compared our results with the predictions of the linear elastic theory. At low forces ($F < 10$–15 pN) the membrane remains in the small deformation limit. A red blood cell membrane may be modeled either by two independent parallel discs if it is in isotonic buffer or by a sphere in hypotonic buffer. In both cases the cell diameter variation is proportional to the applied force, leading to $\mu = 2.5 \pm 0.4$ μN/m. At higher forces we enter the large deformation regime, and we observe deviations from the linear response.

According to our measurements, the value of μ appears to be smaller than the usually accepted one, deduced from micropipette experiments (Evans, 1973; Hochmuth and Waugh, 1987; Lelièvre et al., 1995). A detailed comparison between different methods is presented in the Discussion.

MATERIALS AND METHODS

Red blood cell preparation

Fresh blood was obtained from healthy donors by a fingertip needle prick. Red blood cells (RBCs) were diluted in phosphate-buffered saline (Sigma P 4417) and then washed three times by centrifugation. Whenever necessary, hypotonic buffer (10 mM potassium phosphate, pH 7.4, 75 mM NaCl, i.e., 155 mOsm/kg) was used to get spherical or nearly spherical RBCs.

Silica microbeads, 2.1 μm in diameter, are purchased from Bangs Laboratories (Fishers, IN). The beads were rinsed several times in purified water before addition to the RBC suspension. The added amount corresponded to approximately two beads per erythrocyte. The suspension was then maintained at 4°C for 1 h, allowing spontaneous and nonspecific adhesion of microbeads to the RBC membrane (Svoboda et al., 1992). Finally, it was diluted to ~50,000 RBCs/μl. All observations and measurements were made at room temperature ($T \approx 25$°C).

The embedded observation chamber was made of the usual microscope slide and coverslip, separated by a thin (50 μm) sticking plastic film. At an early stage in the experiment, slides and coverslips were coated with bovine serum albumin (BSA) (Sigma A 4503) to prevent RBC or bead adhesion to glass plates. Actually, we obtained better results using slides silanized with dimethyldichlorosilan. In all cases, a small amount of BSA (~1 mg/ml) is added to the suspension after the beads have stuck to the cells.

Received for publication 10 August 1998 and in final form 10 November 1998.

Address reprint requests to Dr. Sylvie Hénon, Laboratoire de Biorhéologie et d'Hydrodynamique Physico-Chimique, ESA 7057 associée au CNRS et aux Universités Paris 6 et Paris 7, Case courrier 7056, 2 place Jussieu, 75251 Paris cedex 05, France. Tel.: 33-1-44-27-77-82; Fax: 33-1-44-27-43-35; E-mail: henon@lbhp.jussieu.fr.

0006-3495/99/02/1145/07 $2.00

Optics

Our optical tweezers setup is schematized in Fig. 1. It is comparable to the one described with detail by Simmons et al. (1996). We use a noninverted optical microscope (Polyvar model from Reichert) to trap the RBCs and simultaneously observe them. The 1.064 μm Nd:YAG laser beam (model R2-E-106C from Spectra Physics) has a maximum emission power P_{max} = 605 mW. The beam is reflected by a dichroic mirror inside the microscope and focused at the observation point through an immersion objective ($\times$100, numerical aperture 1.25). The wavelength was chosen to minimize water and hemoglobin absorption and to avoid possible damage to the cell. At λ = 1.064 μm, the absorption coefficient for a 2 mM hemoglobin solution is 0.2 cm^{-1} (Svoboda and Block, 1994). From this we estimate a local temperature increase $\Delta T \approx 3°C$ for a red blood cell directly trapped in a 200-mW beam focused over a 1-μm^3 region. This is in agreement with other experimental results and estimates (Liu et al., 1995). The actual heating of the RBCs should be much smaller in our experiment, because we never focus the beam directly on the cell, but on a bead located on its side.

The displacement of the trap in the observation plane is accurately controlled by the rotation of two galvanometric mirrors with perpendicular axes (6800 HP model; Cambridge Technology). By applying a square waveform signal to them, the trap position rapidly commutes between two points, which is equivalent to a pair of traps if the commuting frequency f_c is high enough (current f_c are in the range of 50–300 Hz).

The f = +500 mm converging lens placed between the galvanometric mirrors and the microscope plays two different roles: first it makes the laser beam diameter comparable to the back aperture diameter of the microscope objective, to maximize the beam angular aperture in the observation plane. Second, it conjugates the galvanometric mirrors and this back aperture, so that the laser beam is fully collected by the objective for any angular position of the mirrors.

Force calibrations

The force exerted on a trapped object depends on its size and shape, and on the refractive indices of the object and the surrounding medium. It is proportional to the incident laser power. However, because the sizes of the object and the focusing region are on the same order of magnitude ($\sim$1 μm), it is difficult to calculate *ab initio* the restoring force. Furthermore, because of the optical aberrations of the objective, the exact shape of the trap is not well known. Thus a preliminary force calibration is necessary.

The usual calibration method consists in submitting the trapped spherical bead to a counterflow of known velocity v (Svoboda and Block, 1994; Simmons et al., 1996). The escape force from the trap is exactly opposite the viscous drag force F:

$$F = 6\pi R\eta v \tag{1}$$

where R = 1.05 μm is the bead radius and η is the liquid viscosity. To calibrate a single trap, we apply with one galvanometric mirror a sinusoidal displacement $a = a_0 \sin(2\pi ft)$ to a trapped bead immersed in pure water ($\eta = 0.9\ 10^{-3}$ Pa · s at T = 25°C). For a_0 = 12 μm and in the range $0 < f < 50$ Hz, we observe that the bead always escapes from the trap at the point of maximum velocity $v = 2\pi f a_0$. In this frequency range, the bead inertia is negligible, and at any time the bead velocity has its steady-state value. With f measured as a function of the total laser power P, the escape force $F(P)$ is determined in a first approximation by Eq. 1. Following Svoboda and Block (1994), a correction of order R/d is applied to Eq. 1 to take into account the finite distance d from the bead to the top or bottom of the cell. This correction is larger than 5% only if $d < 10$ μm.

Several calibration curves $F(P)$ are presented in Fig. 2 at different depths of the trap from the top coverslip. As expected, one observes that F is almost a linear function of the power P. At maximum power P_{max} = 605 mW, the escape force may be as high as 80 pN. Nevertheless, there is a slight deviation from the exact proportionality law, for which there are two possible explanations: first the power calibration of the laser may not be quite accurate; second, the spatial mode of the laser is mainly TEM_{00}, but it may be slightly perturbed by other modes at high power, and the trap shape could be affected.

In Fig. 2, one notices that, for a given power P, the force F decreases as the depth h from the top increases. This effect was previously reported by other authors (Svoboda and Block, 1994) and is related to the imperfect stigmatism at distance h from the plane coverslip/water interface. To include this effect, we fit the experimental curves with the empirical calibration formula:

$$F(P, h) = \frac{a_0 + a_1 P + a_2 P^2 + a_3 P^3}{h + h_0} \tag{2}$$

The coefficients a_2 and a_3 account for small corrections to a behavior linear with P. In our case, the agreement with the data is quite satisfying with h_0 = 104.5 μm, as shown in Fig. 2.

We estimate the relative accuracy in the calibration to be $\sim$5%. The main source of uncertainty is the dispersion in bead diameter (estimated to be $\pm$0.1 μm), because we noticed that the escape force for different beads

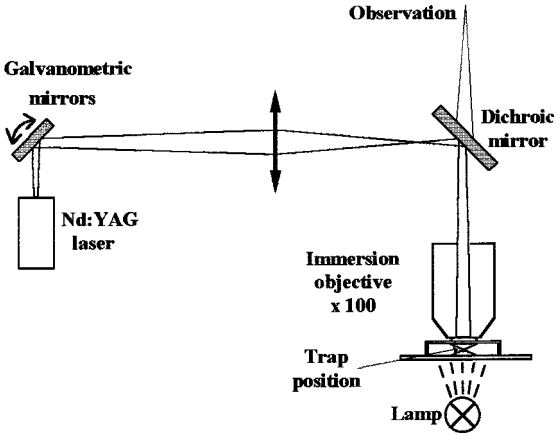

FIGURE 1 Scheme of the optical tweezers experimental setup. Trapping is achieved by focusing the laser beam (λ = 1.064 μm) through the microscope objective. Two perpendicular galvanometric mirrors make it possible to move the trap in the observation plane or split the trap in two by rapidly commuting their position.

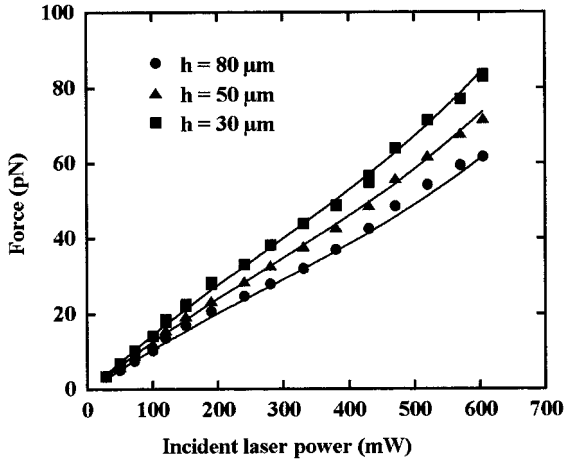

FIGURE 2 Examples of calibration of the escape force of a 2.1-μm silica bead from a single trap F versus the incident laser power P, at different depths h from the top coverslip. Symbols represent experimental data and solid curves are the best interpolation given by the empirical formula (Eq. 2) (see text). Notice that F is roughly proportional to P and decreases with h because of optical aberrations.

trapped in the same conditions may differ by a few percent. Furthermore, small beam misalignment or imperfect cleanliness of optics reduces the escape force by another few percent. Thus we systematically and carefully realign the setup and perform a calibration test before each experiment.

Calibration of the double trap was also necessary for the RBC experiments. Measurements of the escape force F_d from each trap were performed in the same manner as above. We found that $F_d(P, h) = \alpha F(P, h)$, where α is a number of order 0.5, independent of the power P, but slightly dependent on the depth h and on the commutation frequency f_c. We measured, for instance, $\alpha = 0.44$, 0.42, and 0.40, respectively, for $h = 30$, 50, and 80 μm, at the same commutation frequency $f_c = 300$ Hz. The dependence on f_c is hardly significant in the range $50 < f_c < 300$ Hz ($\alpha = 0.46$ for $f_c = 150$ Hz, $h = 30$ μm), but α decreases more rapidly beyond $f_c = 400$ Hz. This is due to the finite commuting time $\Delta t \approx 200$ μs from one trap position to the other.

Experimental procedure, data recording, and analysis

The measurements reported in the following section are made on selected RBCs with two silica beads in diametrical position (see Fig. 3). When the coating of the microscope slide by either BSA or silane is not perfect, it may happen that one of the beads sticks to the bottom glass slide. In this case, we pull on the other free bead with a single trap. In all other cases, we use a double trap to manipulate the cell. Images of the deformed cell are stored with a video cassette recorder and a microcomputer for further analysis. For a given laser power P, we apply an increasing stress to the membrane by slowly incrementing the distance between the two trapped beads. The cell becomes elongated, and its diameter D decreases in the direction perpendicular to the applied force. Just before one of the beads escapes from the trap, we record the cell shape, and we know the applied force F by using the above calibration. By varying the laser power P, we collect a set of images of the same cell submitted to different forces, as shown, for instance, in Fig. 3. If the measurements are quickly repeated, no hysteretic behavior of the shape is observed after the power P is increased and decreased. Actually, when the cell is trapped for several minutes at high power ($P > 300$ mW), some membrane stiffening is observed, and the cell elasticity is affected. Thus we make sure that all of the manipulations on the same cell take place in less than 15 min. Numerical image processing is used to measure the cell diameter D. The border position is located to within ± 1 pixel, and the final accuracy of D is $\sim$100 nm.

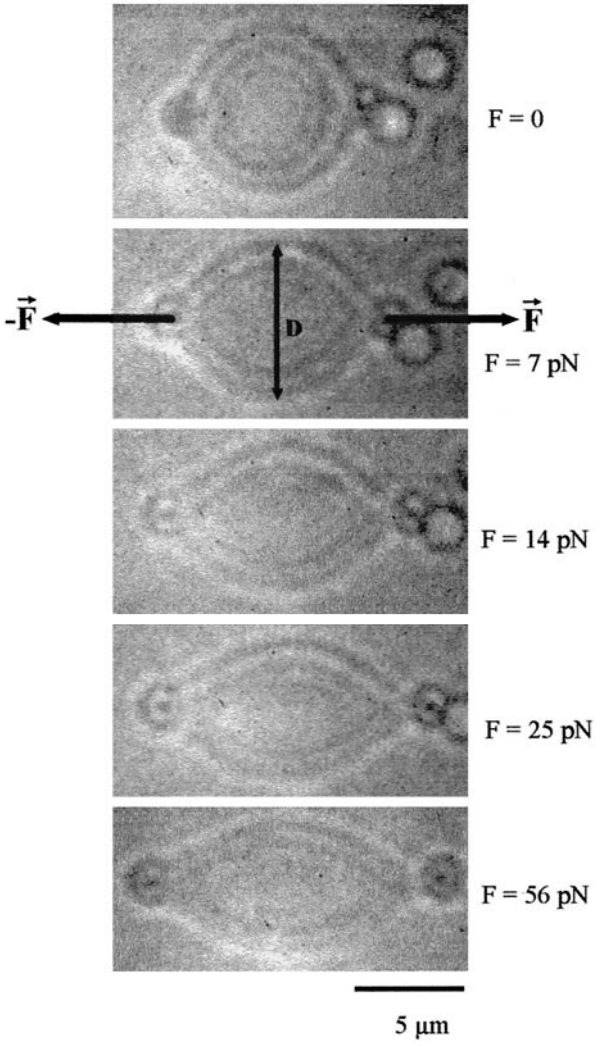

FIGURE 3 Discotic RBC with two silica beads in diametrical position. The deformation increases with increasing force F. Each image is taken just before the bead escapes from the trap, and F is given by the calibration formula (Eq. 2). The variations in diameter D are measured in the direction perpendicular to F.

RESULTS AND DISCUSSION

The inner fluid of the red cell is purely viscous and has no elasticity. As a consequence, the membrane is entirely responsible for the elastic response. In the following, we only consider the linear elasticity limit in the small deformation regime. We assume a constant membrane thickness, which makes the problem purely two-dimensional.

In the small deformation regime, the simple constitutive laws of elasticity are (Landau and Lifshitz, 1959)

$$\begin{aligned} \sigma_{xx} &= K(e_{xx} + e_{yy}) + \mu(e_{xx} - e_{yy}) \\ \sigma_{yy} &= K(e_{xx} + e_{yy}) + \mu(e_{yy} - e_{xx}) \\ \sigma_{xy} &= 2\mu e_{xy} \end{aligned} \tag{3}$$

$\sigma_{ij} = \delta F_i/\delta x_j$ and $e_{ij} = \frac{1}{2}(\delta u_i/\delta x_j + \delta u_j/\delta x_i)$ are the stress and strain tensors (see Fig. 4), K is the area compressibility, and μ is the elastic shear modulus of the membrane.

In a first approximation, the membrane of a discotic unswollen RBC of diameter D_0 at rest is modeled by two parallel independent discs submitted to zero stress at their border. Only two opposite forces of intensity F are exerted

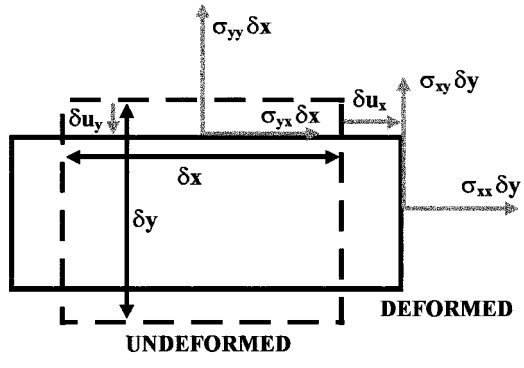

FIGURE 4 Representation of the deformations and stresses exerted on a surface element. It is supposed that the membrane thickness is constant, so that the problem is purely two-dimensional.

at two diametrically opposed points of the disc border. The deformation can be exactly calculated everywhere (Landau and Lifshitz, 1959). In particular, the diameter variation in the direction perpendicular to F is

$$D = D_0 - \frac{F}{2\pi\mu}\left(1 + \left(1 - \frac{\pi}{2}\right)\frac{\mu}{K}\right) \tag{4}$$

The validity of this formula lies in the assumption that there is no stress at the disc border, which is an unverifiable and probably crude approximation. This led us to perform experiments on osmotically swollen spherical or nearly spherical cells as well, because exact algebra can be carried out in this specific geometry.

For a spherical shell with two opposite forces applied at its poles, the stress and deformation are the same along the equator (see Fig. 5):

$$\sigma_{\theta\theta} = \frac{F}{2\pi R} \tag{5a}$$

$$\frac{\sigma_{\theta\theta}}{R'} + \frac{\sigma_{\varphi\varphi}}{R} = 0 \tag{5b}$$

$$\sigma_{\theta\varphi} = 0 \tag{5c}$$

$$e_{\varphi\varphi} = \frac{R - R_0}{R_0} \tag{5d}$$

Here θ and φ are, respectively, the colatitude and azimuth on the sphere, R_0 is the equilibrium radius, and R and R' are the two main radii of curvature at the equator for the deformed sphere. Equation 5b expresses the fact that the membrane is not under tension; there is no pressure difference between the cell interior and exterior.

In the small deformation limit, $R \approx R' \approx R_0$; then $\sigma_{\theta\theta} \approx -\sigma_{\varphi\varphi}$. Equations 3 and 5 lead to

$$D = D_0 - \frac{F}{2\pi\mu} \tag{6}$$

In the case of the RBC membrane, it is often assumed that K is controlled by the phospholipidic bilayer, which has a constant area in a first approximation. On the contrary, μ is determined by the elastic properties of the cytoskeleton, described in the simplest way as a two-dimensional network of spectrin strands bound to the bilayer. It is known from micropipette experiments that K is on the order of 300–500 mN/m (Evans et al., 1976; Waugh and Evans, 1979; Hochmuth and Waugh, 1987), and μ is in the range 4–10 μN/m (Evans, 1973; Hochmuth and Waugh, 1987; Engelhardt and Sackmann, 1988; Lelièvre et al., 1995). Thus the approximation $\mu \ll K$ is generally made for the red blood cell membrane. Within this approximation, Eqs. 4 and 6 take exactly the same form; the expected relation between the deformation and the applied force is the same for discotic and spherical cells.

Actually, it was shown in a recent work (Mohandas and Evans, 1994; Discher et al., 1994) that, because the cytoskeleton is bound to a fluid membrane, it may slip with respect to it. Then an external stress may cause local dilation or compression of the cytoskeleton, although its total area must remain constant, because the phospholipidic bilayer is almost incompressible. This implies that the shear modulus measured in the micropipette experiments is actually a combination of μ and K. For our configuration, in the unrealistic limit where the cytoskeleton would be entirely decoupled from the bilayer, K in Eq. 4 should be replaced by the cytoskeleton elastic constant K_c. Taking the estimate $K_c/\mu \approx 2$ for an ideal triangular spectrin network (Boal et al., 1992; Hansen et al., 1996, and references therein), this would make a 30% difference for the diameter variations between Eqs. 4 and 6. However, because the total area of the cytoskeleton must remain constant, the real effect is smaller. To simplify the following discussion, we decided not to include this effect in Eq. 6, although it should be kept in mind as a possible small correction to our results.

Fig. 6 shows measurements of the diameter D versus applied force F for two RBCs in different buffers: one curve corresponds to a discotic RBC in isotonic conditions, and the other to a swollen RBC in hypotonic buffer. In this last

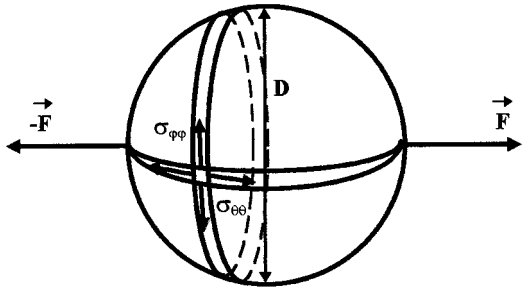

FIGURE 5 Representation of the stresses exerted on a spherical cell by two diametrically opposite forces F. φ is the azimuth and θ the colatitude. $\sigma_{\theta\theta}$ and $\sigma_{\varphi\varphi}$ are constant along any circle parallel to the equator.

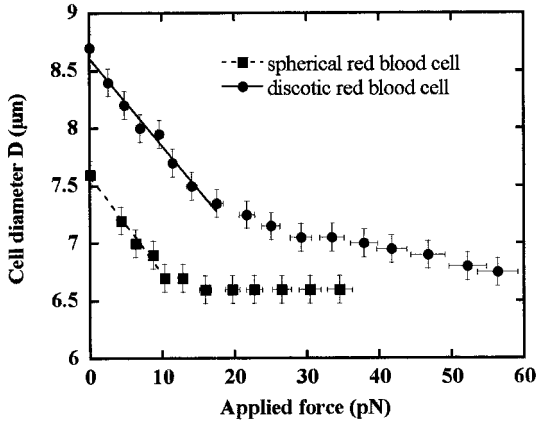

FIGURE 6 Experimental variations of the cell diameter D versus applied force F for a discotic and a quasispherical RBC. The variations are linear at low forces (small deformation), and the membrane shear modulus is given by the slope $D(F)$ in this regime. One finds $\mu = 2.05 \pm 0.3$ μN/m for the discotic cell and $\mu = 1.9 \pm 0.3$ μN/m for the spherical one.

case, the osmolarity is adjusted to make the cell nearly spherical, but to keep the membrane under zero tension at rest. We notice that, in both cases, as long as the force remains small enough (typically $F < 15$ pN), D presents linear variations with F. The shear modulus is deduced from the slope: in these particular cases one finds $\mu = 2.05 \pm 0.3$ μN/m for the discotic cell and $\mu = 1.9 \pm 0.3$ μN/m for the spherical one. At higher forces, one observes deviations from the linear variations, and even a saturation for spherical cells. In the case of discotic cells, the finite deformation regime is reached as soon as $F > 15$ pN. Several models were proposed to describe the membrane elasticity in this regime (Skalak et al., 1973; Evans and Skalak, 1980), and we compared them to our data. Although their predictions somehow differ at large deformation, the shear modulus is only determined by the slope of the curves at small deformation. Thus the value extracted from these models is in agreement with the one above. The case of spherical cells is different: above a force threshold F_c we observe that D remains nearly constant. In Fig. 6, for instance, $F_c = 10$ pN. We interpret this saturation as the effect of an increase in the membrane tension, as soon as the deformation is enough to tighten the membrane.

Fig. 7 shows the histogram of μ measured for 30 discotic and six spherical RBCs. The μ values range from 1.4 to 3.7 μN/m for discotic cells and from 1.7 to 3.3 μN/m for spherical ones. This corresponds to the natural dispersion observed in previous works. The averaged values are $\mu = 2.5 \pm 0.4$ μN/m for discotic and $\mu = 2.35 \pm 0.5$ μN/m for spherical cells. Because no significant difference is found between these two values, we conclude that the shear modulus is the same in the two cases.

Our final result, $\mu = 2.5 \pm 0.4$ μN/m, is comparable to but definitely smaller than previous measurements of μ. An estimate of 10 μN/m for μ was first deduced from the deformation of RBCs in a shear flow (Hochmuth et al., 1973). A widely applied method consists in measuring μ from the length of RBCs aspirated in a micropipette (for instance, Evans, 1973; Hochmuth and Waugh, 1987; Lelièvre et al., 1995); the values obtained with this technique lie between 4 and 10 μN/m, the most commonly accepted value being around 6 μN/m. More recently, the deformation of RBCs in an AC electric field (Engelhardt and Sackmann, 1988) led also to a value of ~6 μN/m. The difference between these results and ours is too large to be due to experimental uncertainties and must necessarily come from the technique itself. Two explanations can be invoked:

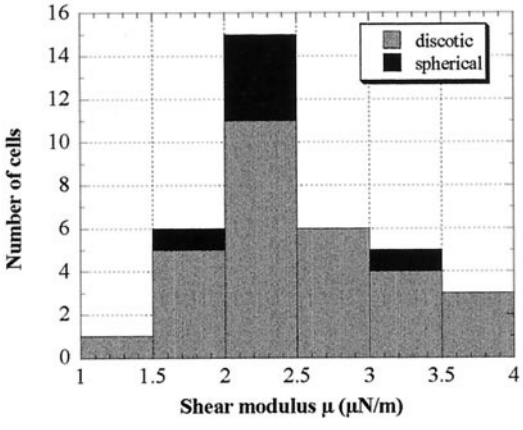

FIGURE 7 Histogram of the shear modulus μ measured for 30 discotic and six quasispherical RBCs. Within experimental error, the averaged μ values for discotic and spherical cells are the same. The final averaged value is $\mu = 2.5 \pm 0.4$ μN/m.

First, these different experiments do not work in the same elasticity regime. With optical tweezers, the cell deformation may be locally large, especially close to the silica beads, but the measurements are taken in the equatorial region, where the deformation always remains small and where the linear theory applies. On the contrary, all other measurements involve the large deformation regime, and their interpretation requires a more complex description than pure linear shear elasticity. Moreover, recent work suggests that a spectrin network may have a nonlinear elastic response and that the elastic coefficients may increase by as much as one order of magnitude from the small to the finite deformation regime (Boal et al., 1992). Our result is consistent with this prediction.

Second, the different techniques may not operate on the same RBC population, at least on average. The optical tweezers technique concerns cells that are tightly bound to glass beads. On the contrary, the micropipette technique supposes that the cells do not adhere to the glass pipette wall, because this would make friction forces play an important role in the force balance. Actually, friction is neglected in the interpretation of micropipette data. Thus one can suppose that these two techniques sort out the cells according to their affinity for glass, which depends on the membrane surface state and which may be associated with different elastic properties from one cell to another.

One could argue that a lower value of the shear modulus may be caused by a heating of the cell or physical or chemical damage of the membrane due to the high laser power. We checked to make sure that this was not the case in our experimental conditions. As we mentioned before, when a 200-mW laser beam is directly focused on the RBC, the temperature elevation in a steady-state regime is only a few degrees. In our setup the beam was not focused on the cell, but on the neighboring beads, and we avoided a total exposure time longer than a few minutes. It is reported in the literature (Waugh and Evans, 1979) that the shear modulus decreases by ~20% when the temperature increases from 25 to 45°C. This effect is definitely too small to account for the difference between the micropipette measurements and ours. Furthermore, we observe no hysteresis when the laser power is cycled between low and high values, which shows that the membrane undergoes no irreversible transformation.

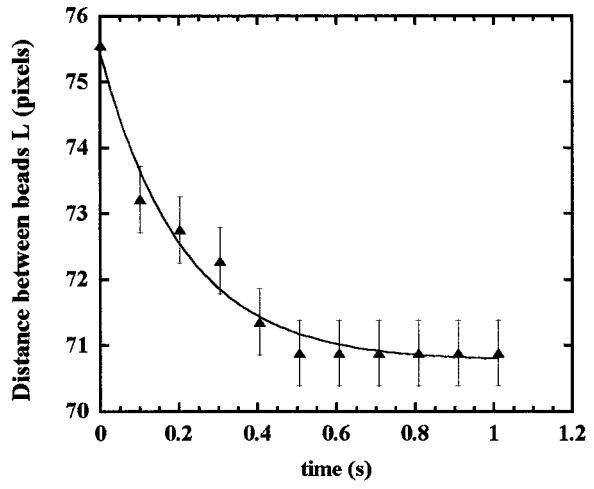

FIGURE 8 Relaxation of an elongated RBC toward equilibrium. The distance $L(t)$ between the two beads bound to the cell is plotted versus time, starting when the cell escapes from the trap. The solid curve represents the best exponential fit, with a time constant $\tau = 206$ ms.

Finally, a good indication that the membrane is not damaged consists in distorting a cell and measuring the relaxation time to its equilibrium shape (Bronkhorst et al., 1995; Linderkamp and Meiselman, 1982; Sutera et al., 1985). This time is controlled by the membrane viscosity and elasticity and varies roughly from 100 ms (young cells) to 300 ms (old cells) in normal conditions (Bronkhorst et al., 1995). Fig. 8 shows an example of the relaxation of a RBC previously elongated by pulling on the beads with the tweezers; the distance $L(t)$ between the two beads is plotted as a function of time. By fitting the data with an exponential curve, the obtained relaxation time in this case is $\tau = 206$ ms. We obtained similar values for all of the RBCs tested by this method. This confirms that in our experiment optical tweezer manipulations have a negligible effect on the cell elastic response.

CONCLUSION

In this paper we showed that, by using silica beads as local handles, optical tweezers are a powerful tool not only for manipulating cells, but also for applying calibrated forces in the pN range. Measuring the induced deformation allows researchers to investigate cell viscoelastic properties. This was applied to the red blood cell membrane; we checked that the method is nonperturbative for the cell and obtained a new determination of the membrane shear modulus μ at small deformations. The measured value $\mu = 2.5 \pm 0.4$ μN/m is about half that measured by the micropipette technique at larger deformations. We argue that there is no contradiction in this statement, because the shear modulus is expected to increase from the small to the finite deformation regime, and because the elastic modulus measured with micropipettes is a combination of the shear modulus and area compressibility.

We acknowledge C. Bucherer, C. Lacombe, N. A. N'Dri, and J. C. Lelièvre for very interesting discussions.

REFERENCES

Ashkin, A., J. M. Dziedzic, and T. Yamane. 1987. Optical trapping and manipulation of single cells using infrared laser beams. *Nature.* 330: 769–771.

Block, S. M., D. F. Blair, and H. C. Berg. 1989. Compliance of bacterial flagella measured with optical tweezers. *Nature.* 338:514–518.

Boal, D. H., U. Seifert, and A. Zilker. 1992. Dual network model for red blood cell membranes. *Phys. Rev. Lett.* 69:3405–09.

Bronkhorst, P. J. H., G. J. Streekstra, J. Grimbergen, E. J. Nijhof, J. J. Sixma, and G. J. Brakenhoff. 1995. A new method to study shape recovery of red blood cells using multiple optical trapping. *Biophys. J.* 69:1666–1673.

Dai, J., and M. P. Sheetz. 1995. Mechanical properties of neuronal growth cone membranes studied by tether formation with laser optical tweezers. *Biophys. J.* 68:988–996.

Discher, D. E., N. Mohandas, and E. A. Evans. 1994. Molecular maps of red cell deformation: hidden elasticity and in situ connectivity. *Science.* 266:1032–1035.

Engelhardt, H., and E. Sackmann. 1988. On the measurement of shear elastic moduli and viscosities of erythrocyte plasma membranes by transient deformation in high frequency electric fields. *Biophys. J.* 54: 495–508.

Evans, E. A. 1973. New membrane concept applied to the analysis of fluid shear- and micropipette-deformed red blood cells. *Biophys. J.* 13: 941–954.

Evans, E. A., and R. Skalak. 1980. Mechanics and Thermodynamics of Biomembranes. CRC Press, Boca Raton, FL.

Evans, E. A., R. Waugh, and L. Melnik. 1976. Elastic area compressibility modulus of red cell membrane. *Biophys. J.* 16:585–595.

Hansen, J. C., R. Skalak, S. Chien, and A. Hoger. 1996. An elastic network model based on the structure of the red blood cell membrane skeleton. *Biophys. J.* 70:146–166.

Hochmuth, R. M., N. Mohandas, and P. L. Blackshear, Jr. 1973. Measurement of the elastic modulus for red cell membrane using a fluid mechanical technique. *Biophys. J.* 13:747–762.

Hochmuth, R. M., and R. E. Waugh. 1987. Erythrocyte membrane elasticity and viscosity. *Annu. Rev. Physiol.* 49:209–219.

Landau, L. D., and E. M. Lifshitz. 1959. Theory of Elasticity. Pergamon Press, New York. 56.

Lelièvre, J. C., C. Bucherer, S. Geiger, C. Lacombe, and V. Vereycken. 1995. Blood cell biomechanics evaluated by the single-cell micromanipulation. *J. Phys. III France.* 5:1689–1706.

Linderkamp, O., and H. J. Meiselman. 1982. Geometric, osmotic, and membrane mechanical properties of density-separated human red cells. *Blood.* 59:1121–1127.

Liu, Y., D. K. Cheng, G. J. Sonek, M. W. Berns, C. F. Chapman, and B. J. Tromberg. 1995. Evidence for localized cell heating induced by infrared optical tweezers. *Biophys. J.* 68:2137–2144.

Mammen, M., K. Helmerson, R. Kishore, S. K. Choi, W. D. Phillips, and G. M. Whitesides. 1996. Optically controlled collisions of biological objects to evaluate potent polyvalent inhibitors of virus-cell adhesion. *Chem. Biol.* 3:757–763.

Mohandas, N., and E. A. Evans. 1994. Mechanical properties of the red cell membrane in relation to molecular structure and genetic defects. *Annu. Rev. Biophys. Biomol. Struct.* 23:787–818.

Simmons, R. M., J. T. Finer, S. Chu, and J. A. Spudich. 1996. Quantitative measurements of force and displacement using optical trap. *Biophys. J.* 70:1813–1822.

Skalak, R., A. Tozeren, R. P. Zarda, and S. Chien. 1973. Strain energy function of red blood cell membranes. *Biophys. J.* 13:245–264.

Sutera, S. P., R. A. Gardner, C. W. Boylan, G. L. Caroll, K. C. Chang, J. S. Marvel, C. Kilo, B. Gonen, and J. R. Williamson. 1985. Age-related changes in deformability of human erythrocytes. *Blood.* 65:275–282.

Svoboda, K., and S. M. Block. 1994. Biological applications of optical forces. *Annu. Rev. Biophys. Biomol. Struct.* 23:247–285.

Svoboda, K., C. F. Schmidt, D. Branton, and S. M. Block. 1992. Conformation and elasticity of the isolated red blood cell membrane skeleton. *Biophys. J.* 63:784–793.

Visscher, K., G. J. Brakenhoff, and J. J. Krol. 1993. Micromanipulation by "multiple" optical traps created by a single fast scanning trap integrated with the bilateral confocal scanning laser microscope. *Cytometry.* 14: 105–114.

Vorobjev, I. A., H. Liang, W. H. Wright, and M. W. Bernes. 1993. Optical trapping for chromosome manipulation: a wave-length dependence of induced chromosome bridges. *Biophys. J.* 64:533–538.

Waugh, R. E., and E. A. Evans. 1979. Thermoelasticity of red blood cell membrane. *Biophys. J.* 26:115–131.